mathematics

MDPI

Article

Chaos Suppression in Uncertain Generalized Lorenz–Stenflo Systems via a Single Rippling Controller with Input Nonlinearity

Chih-Hsueh Lin [1], Guo-Hsin Hu [1,2] and Jun-Juh Yan [3,*]

[1] Department of Electronic Engineering, National Kaohsiung University of Science and Technology, Kaohsiung 80778, Taiwan; cslin@nkust.edu.tw (C.-H.L.); guohsin@mail.mirdc.org.tw (G.-H.H.)
[2] Department of Industrial Upgrading Service, Metal Industries Research & Development Centre, Kaohsiung 81160, Taiwan
[3] Department of Electronic Engineering, National Chin-Yi University of Technology, Taichung 41107, Taiwan
* Correspondence: jjyan@ncut.edu.tw

Received: 22 January 2020; Accepted: 1 March 2020; Published: 3 March 2020

Abstract: In this paper, a robust control design of chaos suppression is considered for generalized four-dimensional (4D) Lorenz–Stenflo systems subjected to matched/mismatched uncertainties and input nonlinearity. It is implemented by using rippling sliding mode control (SMC). A proportional-integral (PI) type scalar switching surface is designed such that the controlled dynamics in the sliding manifold becomes easy to analyze. Furthermore, only by using single rippling SMC even with input nonlinearity can we ensure the existence of the sliding mode for the controlled dynamics and suppress the chaotic behavior in a manner of rippling. Under the proposed control scheme, the chaos behavior in uncertain generalized 4D Lorenz–Stenflo systems subjected to mismatched uncertainties can be robustly suppressed to predictable bounds, which is not addressed in the literature. The numerical simulation results including matched/mismatched uncertainties and nonlinear inputs are presented to verify the robustness and validity of the rippling sliding mode controller.

Keywords: mismatched uncertainty; input nonlinearity; sliding mode control; 4D Lorenz–Stenflo system; rippling control

1. Introduction

Since Lorenz found the famous Lorenz model describing the dynamics of the atmosphere [1], much effort has been devoted to the study of nonlinear chaotic systems. Many fundamental properties can be found in chaotic systems, such as broad spectrums of Fourier transform, strange attractors, excessive sensitivity to initial conditions (so-called butterfly effect), and fractal properties of the state responses [2]. It has also been mentioned that the Lorenz model can depict many different engineering systems, for example, laser devices, the disk dynamics and some issues concerned with convection [3,4]. Due to extensive applications of chaotic systems in solving engineering problems, controlling the complex dynamics of chaotic systems has emerged as an attractive issue for engineering applications and many profound control schemes as well methodologies can be found in the literature [2,5–12]. Consequently, many different effective approaches have been presented to cope with the problems of control and stabilization for various classes of chaotic systems, for example, sliding mode control [5–8], backstepping design [9,10], optimal control [11,12], etc.

In 2017, in order to make more precision models to describe the atmosphere, the authors in [4] proposed a generalized 4D Lorenz–Stenflo system with six parameters. In accordance with the detailed discussion in [13], this proposed generalized Lorenz–Stenflo system has three positive Lyapunov exponents and exhibits interesting and complex chaotic dynamics, since the generalized Lorenz–Stenflo

system is hyper-chaotic in behavior and it is not easy to control, especially when this controlled system is under the influence of external disturbances and nonlinear inputs. In [14], the authors introduced four control inputs to achieve the hyper-chaos suppression. However, the control design cannot apply to the systems which are subjected to external disturbances or nonlinear inputs. Generally, the nonlinearity in the control implementation is highly undesired but always unavoidable due to the physical limitation. If the input nonlinearity is not well taken into account, then it leads system to failure [15,16]. In [17], the authors proposed fuzzy control schemes to control the state variables of the Lorenz–Stenflo chaotic systems to its equilibrium point. By selecting specified parameters, the adaptive controlled system can approach the equilibrium point with high precision. However, the uncertainties considered in [17] need to be dependent on the system states and no clear formula is presented for estimating the control performance. Motivated as mentioned before, the goal of the research is to propose a robust controller to suppress the chaotic behaviors for 4D generalized Lorenz–Stenflo systems subjected to matched/mismatched uncertainties and input nonlinearity. Contrary to previous works [5–12,14] for chaos suppression control, we will consider the input nonlinearity which will always exist in circuit realization for control input. Furthermore, a new control concept called rippling control is introduced for control design. In the rippling control, only certain states of systems are first controlled and, when specified states are suppressed and stabilized, the other states will also be suppressed in the manner of ripple. Thus, the ripple control can not only effectively reduce the number of control inputs but also achieve chaos suppression. Reducing the number of control inputs has remarkable significance in decreasing the complexity of controller realization. Therefore, we will utilize a rippling control method in this research such that only a single control input is used for completing suppression of hyper-chaotic behavior in 4D generalized Lorenz–Stenflo systems even with the undesired input nonlinearity.

The rest of this paper is given as follows. In Section 2, we describe the 4D generalized Lorenz–Stenflo system and formulate the suppression problem of chaos dynamics. In Section 3, integrating the rippling control concept with the sliding mode control, a PI switching surface is designed firstly and the bounds of the controlled chaotic dynamics in the sliding manifold are derived. In Section 4, a rippling sliding mode controller is implemented to achieve the hitting in spite of input with nonlinearity and external disturbances. A procedure for the rippling controller design is proposed. In Section 5, we give the illustrative examples with matched and unmatched conditions, respectively. Finally, conclusions are presented in Section 6.

Notations: In this paper, R^n represents the n-dimensional Euclidean space, R^{nxm} denotes the set of all real n by m matrices, and I_m stands for an m by m identity matrix. $\|W\|$ denotes the Euclidean norm and the induced norm for a matrix W and a vector W, respectively. $|\omega|$ represents the absolute value of ω and $sign(s)$ denotes the sign function of s and we have $sign(s) = 1$ if $s > 0$; $sign(s) = 0$ if $s = 0$; $sign(s) = -1$ if $s < 0$. $diag(\lambda_1, \ldots, \lambda_n) \in R^{n\times n}$ is a diagonal matrix.

2. System and Problem Descriptions

The generalized Lorenz–Stenflo system is described as

$$\begin{aligned} \dot{x}_1(t) &= a(x_2(t) - x_1(t)) + sx_3(t) \\ \dot{x}_2(t) &= cx_1(t) - dx_2(t) - x_1(t)x_4(t) \\ \dot{x}_3(t) &= -x_1(t) - rx_3(t) \\ \dot{x}_4(t) &= x_1(t)x_2(t) - bx_4(t) \end{aligned} \tag{1}$$

where $x_i, i = 1,2,3,4$, are state variables and a, b, c, r, s, d are the system parameters with positive values. System (1) exhibits hyper-chaotic strange attractors, as shown in Figure 1 when $a = 19.42, b = 1.91, c = 29.45, r = 2.86, s = 0.23, d = 9.64$ [4].

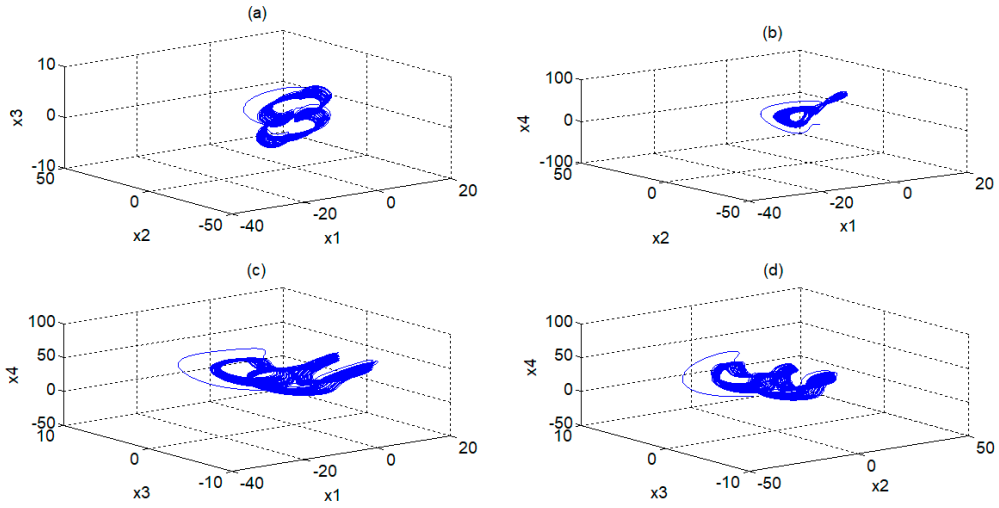

Figure 1. Projection of hyper-chaotic attractor onto (**a**) $x_1 - x_2 - x_3$; (**b**) $x_1 - x_2 - x_4$; (**c**) $x_1 - x_3 - x_4$; (**d**) $x_2 - x_3 - x_4$.

A 4D generalized Lorenz–Stenflo system with mismatched uncertainties can be described as

$$\begin{array}{rcl} \dot{x}_1(t) & = & a(x_2(t) - x_1(t)) + sx_3(t) + \delta_1(t) \\ \dot{x}_2(t) & = & cx_1(t) - dx_2(t) - x_1(t)x_4(t) + \delta_2(t) \\ \dot{x}_3(t) & = & -x_1(t) - rx_3(t) + \delta_3(t) \\ \dot{x}_4(t) & = & x_1(t)x_2(t) - bx_4(t) + \delta_4(t) \end{array} \tag{2}$$

Generally, the considered uncertainties $\delta_i(t),\ i\ =\ 1,2,3,4$ in (2) are bounded by

$$\left|\delta_i(t)\right| \leq \rho_i, i\ =\ 1,2,3,4,\ \text{for all time } t \tag{3}$$

where $\rho_i \geq 0$ are given. For effectively controlling the uncertain system (2), we introduce a controller $u(t)$ to the system (2). After introducing this single input subjected to input nonlinearity, the controlled system can be expressed by

$$\begin{array}{rcl} \dot{x}_1(t) & = & a(x_2(t) - x_1(t)) + sx_3(t) + \delta_1(t) \\ \dot{x}_2(t) & = & cx_1(t) - dx_2(t) - x_1(t)x_4(t) + \delta_2(t) + \phi(u(t)) \\ \dot{x}_3(t) & = & -x_1(t) - rx_3(t) + \delta_3(t) \\ \dot{x}_4(t) & = & x_1(t)x_2(t) - bx_4(t) + \delta_4(t) \end{array} \tag{4}$$

where $u(t) \in R$ denotes the control input, $\phi(u(t)) \in R$ is the control input with nonlinearity. The nonlinear input $\phi(u(t))$ satisfies $\phi(0)\ =\ 0$, $\phi(u(t)) \in R \to R$ and is bounded in the sector $[\alpha_2,\ \alpha_1]$, the α_1 and α_2 are the known positive constants. Therefore, it can be formulated as

$$\alpha_2 u^2 \geq u\phi(u(t)) \geq \alpha_1 u^2 \tag{5}$$

The nonlinear control input $\phi(u(t))$ is shown in Figure 2.

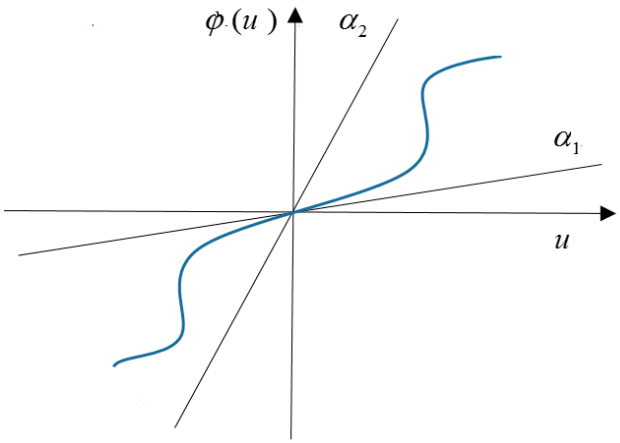

Figure 2. The nonlinear control input within the bounded sector $[\alpha_2,\ \alpha_1]$.

The goal of this paper is to propose a single rippling SMC to suppress the chaos behavior in the uncertain 4D Lorenz–Stenflo system to zero or predictable bounds even with mismatched uncertainties and input nonlinearity, i.e.,

$$\lim_{t\to\infty}\left|x_i(t)\right| \le \psi_i, i \ = \ 1,2,3,4 \tag{6}$$

where $\psi_i \ge 0$ are the upper bounds estimated which will depend on external uncertainties.

By utilizing the sliding mode control technology to achieve our control goal, two major problems need to be solved well. First, we need to decide a proper switching surface for the controlled system (4) to ensure that the dynamics in the sliding manifold have predicted bounds with $\lim_{t\to\infty}|x_i| \le \psi_i, i \ = \ 1,2,3,4$ even under the influence of external uncertainties. Next, we need to determine a sliding mode controller such that the trajectory of controlled system (4) can be driven to the switching surface even with the nonlinearity of gain reduction tolerance in the control input.

3. PI Switching Function and Estimated State Bounds in the Sliding Manifold

In this section, we will propose the design procedures of the controller. To reduce the number of control inputs, we introduce the concept of the rippling control and only the first three states $x_i, i \ = \ 1,2,3$ of the system in (4) are controlled. When the specified states are suppressed and stabilized, the fourth state x_4 will also be suppressed in the manner of ripple. Therefore, we first select a proper switching surface which is only relative in the first three states $x_i, i \ = \ 1,2,3$ of system in (4) to ensure the control performance in the sliding manifold; then, a robust SMC is developed to guarantee the hitting of the sliding mode manifold even with matched/unmatched uncertainties and input nonlinearity. The proportional-integral (PI) switching surface is selected as

$$\sigma(t) \ = \ x_2(t) + \int_0^t KV(\tau)d\tau \tag{7}$$

where $\sigma(t) \in R$, $V(t) \ = \ \begin{bmatrix} x_1(t) & x_2(t) & x_3(t) \end{bmatrix}^T$, $K \ = \ \begin{bmatrix} k_1 & k_2 & k_3 \end{bmatrix} \in R^{1\times 3}$ is a designed gain matrix that can be easily determined later. Assuming that the system operates in the sliding mode when $t \ge t_s$, according to the sliding mode control theorem, the equivalent control law can be obtained due to the facts of $s(t) \ = \ 0$ and $\dot{s}(t) \ = \ 0$. Considering (7) and (4), we have

$$\begin{aligned} \dot{\sigma}(t) \ &= \dot{x}_2(t) + KV(t) \\ &= cx_1(t) - dx_2(t) - x_1(t)x_4(t) + \delta_2(t) + \phi(u(t)) + KV(t). \end{aligned} \tag{8}$$

From (8), if the controlled system is in the sliding manifold, we have $s(t) = \dot{s}(t) = 0$ and the equivalent control law can be obtained as

$$\phi_{eq}(u(t)) = -(cx_1(t) - dx_2(t) - x_1(t)x_4(t) + \delta_2(t)) - KV(t) \tag{9}$$

Substituting (9) into (4) yields

$$\begin{array}{rcl} \dot{x}_1(t) & = & a(x_2(t) - x_1(t)) + sx_3(t) + \delta_1(t) \\ \dot{x}_2(t) & = & -k_1x_1(t) - k_2x_2(t) - k_3x_3(t) = -KV(t) \\ \dot{x}_3(t) & = & -x_1(t) - rx_3(t) + \delta_3(t) \\ \dot{x}_4(t) & = & x_1(t)x_2(t) - bx_4(t) + \delta_4(t) \end{array} \tag{10}$$

Rearranging the differential equations for the first three states in (10), we have

$$\dot{V}(t) = \begin{bmatrix} \dot{x}_1(t) \\ \dot{x}_2(t) \\ \dot{x}_3(t) \end{bmatrix} = \hat{A}V(t) + \delta(t) \tag{11}$$

where $A = \begin{bmatrix} -a & a & s \\ 0 & 0 & 0 \\ -1 & 0 & -r \end{bmatrix}, B = \begin{bmatrix} 0 \\ 1 \\ 0 \end{bmatrix}, \hat{A} = A - BK, \delta(t) = \begin{bmatrix} \delta_1(t) \\ 0 \\ \delta_3(t) \end{bmatrix}$.

Since (A, B) is controllable, we can always select a specified gain matrix K by using any pole assignment method such that eigenvalues $\lambda_i, i = 1, 2, 3$ of matrix $\hat{A}$ are all different and satisfy $\lambda_i < 0, i = 1, 2, 3$.

Solving (11), one has for $t \geq t_s$

$$V(t) = \begin{bmatrix} x_1(t) \\ x_2(t) \\ x_3(t) \end{bmatrix} = e^{\hat{A}(t-t_s)}V(t_s) + \int_{t_s}^{t} e^{\hat{A}(t-\tau)}\delta(\tau)d\tau \tag{12}$$

Now, selecting $P = \begin{bmatrix} p_1 & p_2 & p_3 \end{bmatrix} \in R^{3\times3}$ to satisfy $\hat{A} = P\Lambda P^{-1}, \Lambda = diag(\lambda_1, \lambda_2, \lambda_3), p_i \in R^{3\times1}$ is the independent eigenvector corresponding to eigenvalue λ_i of matrix $\hat{A}$.

Since $e^{\hat{A}t} = Pe^{\Lambda t}P^{-1}$, one has

$$V(t) = \begin{bmatrix} x_1(t) \\ x_2(t) \\ x_3(t) \end{bmatrix} = Pe^{\Lambda(t-t_s)}P^{-1}V(t_s) + \int_{t_s}^{t} Pe^{\Lambda(t-\tau)}P^{-1}\delta(\tau)d\tau \tag{13}$$

and the solution of $x_i(t), i = 1, 2, 3$ can be obtained as

$$x_i(t) = \theta_i V(t) = \theta_i Pe^{\Lambda(t-t_s)}P^{-1}V(t_s) + \int_{t_s}^{t} \theta_i Pe^{\Lambda(t-\tau)}P^{-1}\delta(\tau)d\tau \tag{14}$$

where θ_i is i-row of I_3.

The bounds of $x_i(t), i = 1, 2, 3$, for $t \geq t_s$, can be estimated by

$$\begin{array}{rl} \left|x_i(t)\right| & = \left|\theta_i Pe^{\Lambda(t-t_s)}P^{-1}V(t_s) + \int_{t_s}^{t} \theta_i Pe^{\Lambda(t-\tau)}P^{-1}\delta(\tau)d\tau\right| \\ & \leq \left|\theta_i Pe^{\Lambda(t-t_s)}P^{-1}V(t_s)\right| + \left|\int_{t_s}^{t} \theta_i Pe^{\Lambda(t-\tau)}P^{-1}\delta(\tau)d\tau\right|. \end{array} \tag{15}$$

The definite integral of $\int_{t_s}^{t} \theta_i P e^{\Lambda(t-\tau)} P^{-1} \delta(\tau) d\tau$ in (15) can be represented by the limit of the Riemann sum [18] described as below:

$$\int_{t_s}^{t} \theta_i P e^{\Lambda(t-\tau)} P^{-1} \delta(\tau) d\tau \;=\; \lim_{n\to\infty} \sum_{i=1}^{n} \theta_i P e^{\Lambda(t-t^*)} P^{-1} \delta(t^*) \Delta\tau \tag{16}$$

where $\Delta\tau \;=\; \frac{t-t_s}{n} > 0$ and $t^* \;=\; t_s + \Delta\tau \cdot i$.

Therefore, we have

$$\begin{aligned}
&\left|\int_{t_s}^{t} \theta_i P e^{\Lambda(t-\tau)} P^{-1} \delta(\tau) d\tau\right| \\
&= \left|\lim_{n\to\infty} \sum_{i=1}^{n} \theta_i P e^{\Lambda(t-t^*)} P^{-1} \delta(t^*) \Delta\tau\right| \\
&= \left|\lim_{n\to\infty} \theta_i P \sum_{i=1}^{n} e^{\Lambda(t-t^*)} P^{-1} \Delta\tau \delta(t^*)\right| \\
&\le \left|\| \theta_i P \lim_{n\to\infty} \sum_{i=1}^{n} e^{\Lambda(t-t^*)} P^{-1} \Delta\tau \,\|\|\, \delta(t^*) \,\|\right| \\
&\le \left|\| \theta_i P \lim_{n\to\infty} \sum_{i=1}^{n} e^{\Lambda(t-t^*)} \Delta\tau P^{-1} \,\| \max_{t\ge t_s} \| \,\delta(t) \,\|\right| \;=\; \| \,\theta_i P \int_{t_s}^{t} e^{\Lambda(t-\tau)} d\tau P^{-1} \,\| \max_{t\ge t_s} \| \,\delta(t) \,\|.
\end{aligned} \tag{17}$$

By substituting (17) into (15), we have

$$\begin{aligned}
\left|x_i(t)\right| &\le \left|\theta_i P e^{\Lambda(t-t_s)} P^{-1} V(t_s)\right| + \| \,\theta_i P \int_{t_s}^{t} e^{\Lambda(t-\tau)} d\tau P^{-1} \,\| \max_{t\ge t_s} \| \,\delta(t) \,\| \\
&\le \left|\theta_i P e^{\Lambda(t-t_s)} P^{-1} V(t_s)\right| + \| \,\theta_i P diag\left(\frac{e^{\lambda_1(t-\tau)}}{-\lambda_1}, \frac{e^{\lambda_2(t-\tau)}}{-\lambda_2}, \frac{e^{\lambda_3(t-\tau)}}{-\lambda_3}\right)\Big|_{\tau\;=\;t_s}^{\tau\;=\;t} P^{-1} \,\|(\max_{t\ge t_s} \| \,\delta(t) \,\|) \\
&\le \left|\theta_i P e^{\Lambda(t-t_s)} P^{-1} V(t_s)\right| + \| \,\theta_i P diag\left(-\frac{1}{\lambda_1} + \frac{e^{\lambda_1(t-t_s)}}{\lambda_1}, -\frac{1}{\lambda_2} + \frac{e^{\lambda_2(t-t_s)}}{\lambda_2}, -\frac{1}{\lambda_3} + \frac{e^{\lambda_3(t-t_s)}}{\lambda_3}\right) P^{-1} \,\|(\max_{t\ge t_s} \| \,\delta(t) \,\|)
\end{aligned} \tag{18}$$

Since $\lambda_i \;<\; 0, i \;=\; 1,2,3$ and $\max_{t\ge t_s}\|\delta(t)\| \;=\; \max_{t\ge t_s}\|\begin{bmatrix} \delta_1(t) & 0 & \delta_3(t) \end{bmatrix}^T\| \;\le\; \max_{t\ge t_s}(\left|\delta_1(t)\right| + \left|\delta_3(t)\right|) \;=\; \rho_1 + \rho_3$, we have the bounds ψ_i of $x_i(t), i \;=\; 1,2,3$ as

$$\begin{aligned}
\psi_i \;&= \lim_{t\to\infty}\left|x_i(t)\right| \le \lim_{t\to\infty}\left|\theta_i P e^{\Lambda(t-t_s)} P^{-1} V(t_s)\right| \\
&+ \lim_{t\to\infty}\|\theta_i P diag(-\tfrac{1}{\lambda_1} + \tfrac{e^{\lambda_1(t-t_s)}}{\lambda_1}, -\tfrac{1}{\lambda_2} + \tfrac{e^{\lambda_2(t-t_s)}}{\lambda_2}, -\tfrac{1}{\lambda_3} + \tfrac{e^{\lambda_3(t-t_s)}}{\lambda_3}) P^{-1}\|(\max_{t\ge t_s}\|\delta(t)\|) \\
&\le \|\theta_i P diag(\tfrac{1}{\lambda_1}, \tfrac{1}{\lambda_2}, \tfrac{1}{\lambda_3}) P^{-1}\|(\rho_1 + \rho_3).
\end{aligned} \tag{19}$$

Similarly, from (2), since $b > 0$, we can calculate $\psi_4 \;=\; \lim_{t\to\infty}\left|x_4(t)\right|$ as

$$\begin{aligned}
\psi_4 \;&= \lim_{t\to\infty}\left|x_4(t)\right| \le \lim_{t\to\infty}\left|e^{-bt} x_4(0)\right| + \tfrac{1}{b}\lim_{t\to\infty}(\left|\delta_4(t)\right| + \left|x_1(t)x_2(t)\right|) \\
&\le \tfrac{1}{b}(\rho_4 + \psi_1\psi_2).
\end{aligned} \tag{20}$$

Remark 1. *For the system with $\delta_i \;=\; 0, i \;=\; 1,3,4$, according to (19) and (20), we can conclude that when system (4) enters the sliding manifold, all controlled states will be forced to zero, i.e., $\lim_{t\to\infty}|x_i| \;=\; 0, i \;=\; 1,2,3,4$, even with the matched uncertainty $\delta_2(t) \neq 0$.*

Although we have estimated the state bounds of controlled dynamics in the sliding manifold, we still need to determine a control input such that the controlled system can be driven to the switching surface and the existence of the sliding motion can be guaranteed even with the gain reduction tolerance in the control input.

4. Robust Controller Design for Sliding Motion

In order to design the SMC scheme, the hitting condition is given below.

Lemma 1. *The trajectory of controlled systems can converge to the sliding mode (7), i.e.,* $\sigma(t) = 0$, *if the following hitting condition is satisfied:*

$$\sigma(t)\dot{\sigma}(t) < 0 \tag{21}$$

Proof of Lemma 1. Let $v(t) = \frac{1}{2}\sigma^2(t) > 0$, for all $\sigma(t) \neq 0$, be the Lyapunov function. From the Lyapunov stability theory, condition (21) implies $\dot{v}(t) = \sigma(t)\dot{\sigma}(t) < 0$ and $v(t)$ as well as that the switching function $\sigma(t)$ can converge to zero. □

To achieve the reaching condition indicated in Lemma 1, the control input subjected to input nonlinearity is proposed as

$$u(t) = -\eta(\left|cx_1(t) - dx_2(t) - x_1(t)x_4(t) + KV(t)\right| + \rho_2)sign(\sigma(t)),\ \eta > \alpha_1^{-1} \tag{22}$$

In the following, we will prove that the proposed scheme (19) can drive the uncertain system (4) with input nonlinearity onto the sliding mode $\sigma(t) = 0$.

Theorem 1. *Considering that the uncertain system (4) with input nonlinearity, let the control* $u(t)$ *be given as (22), then, the system trajectory asymptotically converges to the sliding manifold* $\sigma(t) = 0$.

Proof of Theorem 1. Substituting (4) and the control (22) into the derivative $\dot{\sigma}(t)\sigma(t)$, we obtain

$$\begin{aligned} &\sigma(t)\dot{\sigma}(t) = \sigma(t)(\dot{x}_2(t) + KV(t)) \\ &= \sigma(t)(cx_1(t) - dx_2(t) - x_1(t)x_4(t) + \delta_2(t) + \phi(u(t)) + KV(t)) \\ &\leq \left|\sigma(t)\right|(\left|cx_1(t) - dx_2(t) - x_1(t)x_4(t) + KV(t)\right| + \rho_2) + \sigma(t)\phi(u(t)). \end{aligned} \tag{23}$$

By using (5), one has

$$\begin{aligned} &u(t)\phi(u(t)) = -\eta(\left|cx_1(t) - dx_2(t) - x_1(t)x_4(t) + KV(t)\right| + \rho_2)sign(\sigma(t))\phi(u(t)) \\ &\geq \alpha_1 u^2(t) = \alpha_1\eta^2(\left|cx_1(t) - dx_2(t) - x_1(t)x_4(t) + KV(t)\right| + \rho_2)^2 sign^2(\sigma(t))\phi(u(t)). \end{aligned} \tag{24}$$

Furthermore, by multiplying $\sigma^2(t) \geq 0$ to (24) and using the fact of $\sigma(t)sign((t)) = \left|\sigma(t)\right|$, we have

$$\begin{aligned} &-\eta(\left|cx_1(t) - dx_2(t) - x_1(t)x_4(t) + KV(t)\right| + \rho_2)\sigma(t)\left|\sigma(t)\right|\phi(u(t)) \\ &\geq \alpha_1\eta^2(\left|cx_1(t) - dx_2(t) - x_1(t)x_4(t) + KV(t)\right| + \rho_2)^2\left|\sigma(t)\right|^2. \end{aligned} \tag{25}$$

From (25), we can further derive

$$\sigma(t)\phi(u(t)) \leq -\alpha_1\eta(\left|cx_1(t) - dx_2(t) - x_1(t)x_4(t) + KV(t)\right| + \rho_2)\left|\sigma(t)\right|. \tag{26}$$

Since $\eta > \alpha^{-1}$, combined with (26), (23) yields

$$\sigma(t)\dot{\sigma}(t) \leq (1 - \eta\alpha)\ (\left|cx_1(t) - dx_2(t) - x_1(t)x_4(t) + KV(t)\right| + \rho_2)\left|\sigma(t)\right| < 0. \tag{27}$$

Thus, according to Lemma 1, one can conclude that the system trajectory asymptotically converges to the sliding manifold $\sigma(t) = 0$. □

Remark 2. *From the theoretical point of view, the proposed control input (22) may result in chattering due to the discontinuous sign function. A simple approach to solve this problem is to modify the controller (22) as*

$$u(t) = -\eta(\left|cx_1(t) - dx_2(t) - x_1(t)x_4(t) + KV(t)\right| + \rho_2)\frac{\sigma(t)}{\left|\sigma(t)\right| + \varepsilon} \tag{28}$$

where ε is a sufficiently small positive constant. Obviously, the continuous controller (28) with a sufficiently small value of ε can approach the discontinuous controller (22) very well.

We can systematize the design procedure for robust chaos synchronization as follows.

Remark 3. *According to the above discussion, we can systematize the design procedure for robust chaos suppression in generalized 4D Lorenz–Stenflo systems as follows.*

Step 1: Select the gain matrix K to guarantee that the eigenvalues $\lambda_i, i = 1, 2, 3$ of matrix $\hat{A}$ in (11) are all different and satisfy $\lambda_i < 0, i = 1, 2, 3$, which will ensure a stable sliding manifold.

Step 2: Construct the switching function $\sigma(t)$ in (7).

Step 3: Find independent eigenvectors corresponding to eigenvalue λ_i of matrix $\hat{A}$ and construct the transform matrix P.

Step4: Obtain the predicted error bounds $\psi_i, i = 1, 2, 3, 4$ by using (19) and (20).

Step5: Construct the SMC from (22) or (28).

5. Numerical Simulations

In this example, in the generalized 4D Lorenz–Stenflo system (1), the six parameters are selected as $a = 19.42, b = 1.91, c = 29.45, r = 2.86, s = 0.23, d = 9.64$. We can easily check that the pair (A, B) is controllable and, according to Step 1 in Remark 3, we can easily select the gain matrix $K = [\ 7.7892 \quad -4.6500 \quad -7.7654]$ such that $\lambda_1 = -6, \lambda_2 = -5, \lambda_3 = -4$ to result in a stable sliding motion. According to (7), the switching function $\sigma(t)$ can be obtained as

$$\sigma(t) = x_2(t) + \int_0^t ([\ 7.7892 \quad -4.6500 \quad -7.7654]\begin{bmatrix} x_1(\tau) \\ x_2(\tau) \\ x_3(\tau) \end{bmatrix})d\tau \tag{29}$$

and the transform matrix $P = \begin{bmatrix} 0.8463 & -0.8300 & 0.8140 \\ 0.5120 & -0.5299 & 0.5392 \\ 0.1467 & -0.1740 & 0.2159 \end{bmatrix}$

For simulation, we define the nonlinear input as $\phi(u(t)) = (1 + 0.2\sin(5x_1(t)))u(t)$. Obviously, we can obtain $u(t)\phi(u(t)) \geq 0.8u^2(t)$ and $\alpha_1 = 0.8$. The sliding mode controller can be constructed as

$$u(t) = -\eta(\left|cx_1(t) - dx_2(t) - x_1(t)x_4(t) + KV(t)\right| + \rho_2)\frac{\sigma(t)}{\left|\sigma(t)\right| + \varepsilon} \tag{30}$$

with $\eta = 2 > \frac{1}{0.8}, \varepsilon = 0.02$.

In the following, numerical experiments including matched and unmatched conditions of uncertainties are given to verify the control performance of the present SMC design.

5.1. Robust Control with Matched Uncertainty and Input Nonlinearity

The unmatched uncertainties are set as $\delta_1(t) = \delta_3(t) = \delta_4(t) = 0$. The matched uncertainty is given as $\delta_2(t) = 0.3\sin(2t)$. In this simulation, we enable the control input at $t = 3$ s. According to (19) and (20), we can understand that the controlled system states will be exactly driven to zero. Figures 3 and 4 show the simulation results with initial condition $(x_1(0), x_2(0), x_3(0), x_4(0)) = (1, -3, 2, -5)$.

Figure 3 shows the state responses under the proposed controller (30). Figure 4a,b, respectively, show the corresponding $\sigma(t)$ for the controlled 4D Lorenz–Stenflo system and the control input for $t \geq 3$ s. By observing the simulation results, it reveals that the controlled trajectory of the system hits $\sigma(t) = 0$ at $t = 3.3$ s. and the states approach to zero after $t = 5.5$, i.e., the system state is exactly forced to zero and the proposed SMC (30) is robust to the matched uncertainty and input nonlinearity.

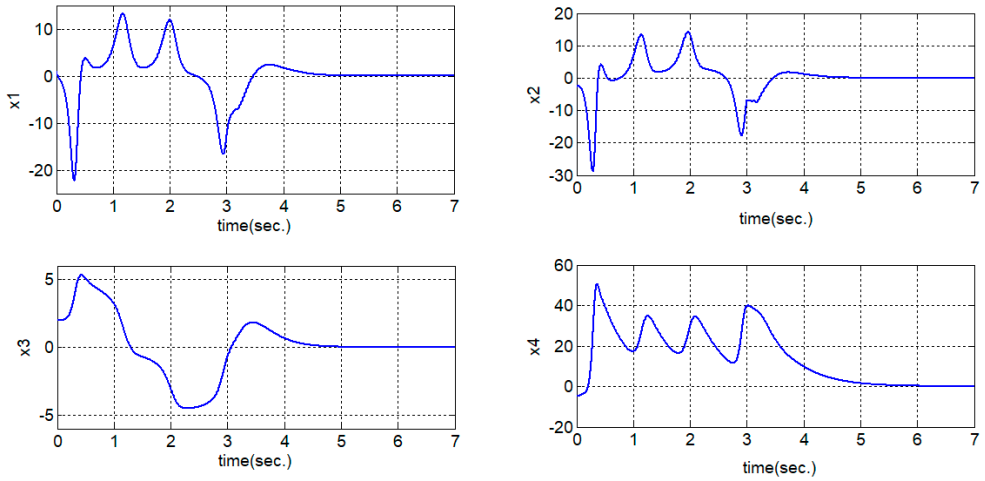

Figure 3. The state responses of the controlled system with the SMC (30). (The controller is active when $t \geq 3$ s).

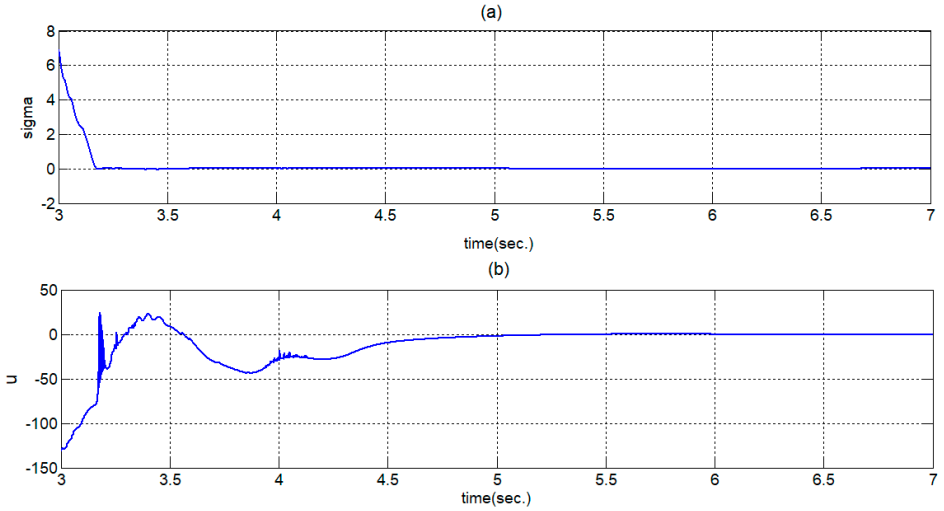

Figure 4. (**a**) time response of switching function $\sigma(t)$; (**b**) time response of control input $u(t)$; the controller is active when $t \geq 3$ s.

5.2. Robust Control with Mismatch Uncertainties and Input Nonlinearity

Here, we consider the control performance under the influence of mismatch external uncertainties $\delta_1(t) = 0.2\cos(2t), \delta_2(t) = \sin(t), \delta_3(t) = 0.5\cos(2t), \delta_4(t) = 0.5\sin(8t)$. The control input becomes active at $t = 6$ s.

Obviously, we have $|\delta_1(t)| \leq \rho_1 = 0.2, |\delta_2(t)| \leq \rho_2 = 1, |\delta_3(t)| \leq \rho_3 = 0.3, |\delta_4(t)| \leq \rho_4 = 0.8$. Furthermore, by Equations (19) and (20), we can calculate that the controlled states are bounded by $\psi_1 = 0.6188, \psi_2 = 0.4527, \psi_3 = 0.2673, \psi_4 = 0.5655$.

The initial condition $(x_1(0), x_2(0), x_3(0), x_4(0)) = (1, -3, 2, -2)$ is used in this simulation. The state responses are shown in Figure 5. The detailed state responses for $t \geq 10$ s are shown in Figure 6 to get a clearer view. According to Figure 6, it reveals that the controlled states are suppressed and bounded by $\psi_i, i = 1, 2, 3, 4$, as we estimate with (19) and (20). Figure 7a,b, respectively, show the

corresponding $\sigma(t)$ and the control input for $t \geq 6$ s. From Figure 7b, it can be observed that the chattering phenomenon can disappear when $t \geq 7.5$ s.

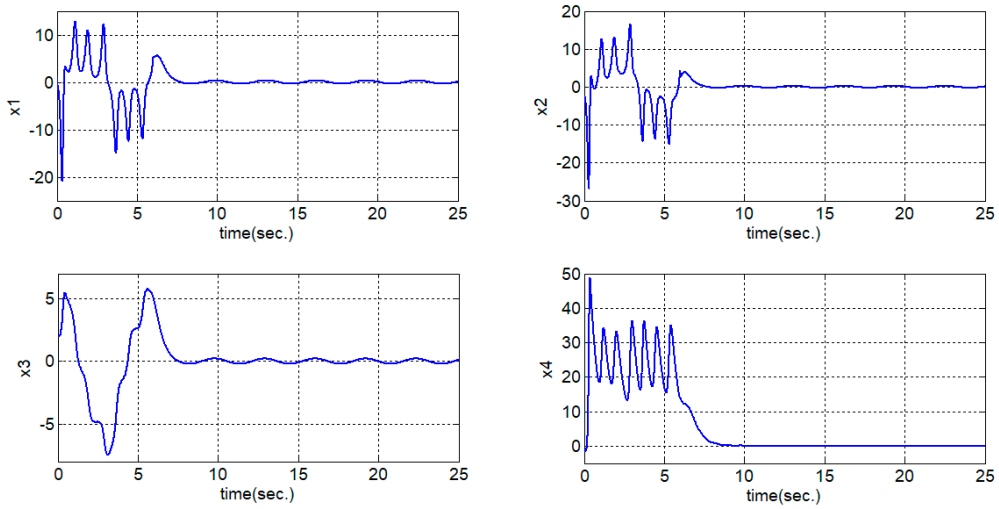

Figure 5. State responses of the controlled system with unmatched uncertainties (the controller is enabled when $t \geq 6$ s).

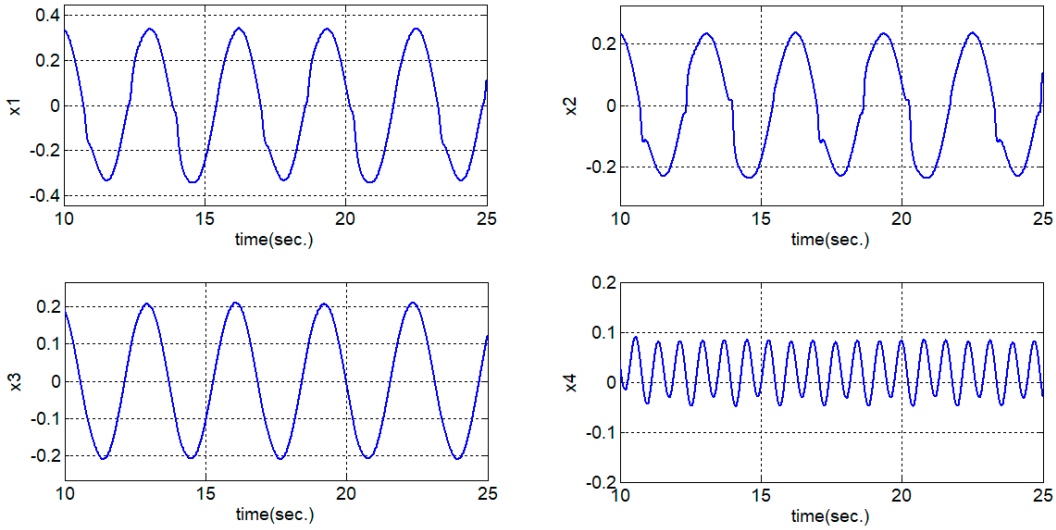

Figure 6. The detailed state responses of the controlled system for $t \geq 10$ s.

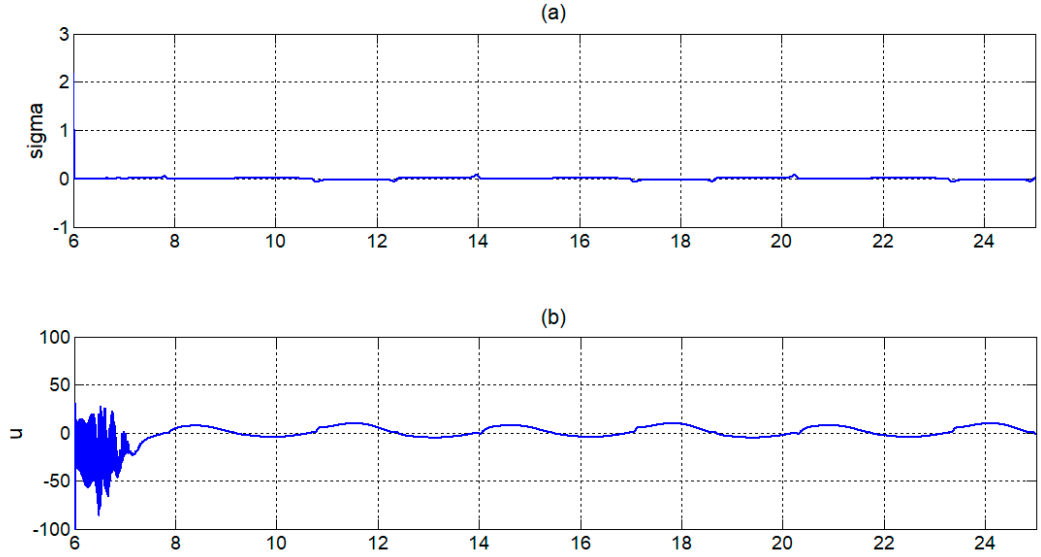

Figure 7. (**a**) time response of switching function $\sigma(t)$; (**b**) time response of control input $u(t)$; the controller is active when $t \geq 6$ s.

6. Conclusions

A robust chaos suppression control for 4D generalized Lorenz–Stenflo systems subject to matched/mismatched uncertainties and input nonlinearity is proposed in this paper. A new rippling sliding mode controller has been developed to regulate the state vector. According to the mathematical analysis and simulation results, we can observe that the proposed sliding mode controller is effective for controlling uncertain 4D generalized Lorenz–Stenflo systems even with matched/mismatched uncertainties as well as input nonlinearity. Moreover, the bounds of controlled system states have also been well discussed under the effect of mismatch uncertainties. The numerical simulation results demonstrate the robustness and validity of the proposed chaos suppression controller. In the near future, our main work is to extend the proposed rippling sliding mode control to suppress the stochastic chaos systems with multiplicative noises.

Author Contributions: All authors contributed to this manuscript. G.-H.H. wrote the paper with supervision from C.-H.L. and J.-J.Y., and G.-H.H. was responsible for the simulation program design of the robust rippling sliding mode control. All authors have read and agreed to the published version of the manuscript.

Funding: This work was financially supported by the Ministry of Science and Technology, Taiwan, under MOST-107-2221-E-167-032-MY2.

Conflicts of Interest: The authors declare no conflict of interest.

References

1. Lorenz, E.N. Deterministic nonperiodic flow. *J. Atmos. Sci.* **1963**, *20*, 130–141. [CrossRef]
2. Yan, J.J.; Liao, T.L. Discrete sliding mode control for hybrid synchronization of continuous Lorenz systems with matched/unmatched disturbances. *Trans. Inst. Meas. Control.* **2018**, *40*, 1417–1424. [CrossRef]
3. Zhang, F.; Xiao, M. Complex Dynamical Behaviors of Lorenz–Stenflo Equations. *Mathematics* **2019**, *7*, 513. [CrossRef]
4. Chen, Y.M.; Liang, H.H. Zero-zero-Hopf bifurcation and ultimate bound estimation of a generalized Lorenz–Stenflo hyperchaotic system. *Math. Method Appl. Sci.* **2017**, *40*, 3424–3432. [CrossRef]
5. Arjmand, M.T.; Sadeghian, H.; Salarieh, H.; Alasty, A. Chaos control in AFM systems using nonlinear delayed feedback via sliding mode control. *Nonlinear Anal. Hybrid Syst.* **2008**, *2*, 993–1001. [CrossRef]
6. Wang, C.C.; Yau, H.T. Nonlinear dynamic analysis and sliding mode control for a gyroscope system. *Nonlinear Dynam.* **2011**, *66*, 53–65. [CrossRef]

7. Zribi, M.; Alrifai, M.T.; Smaoui, N. Control of Chaos in a Single Machine Infinite Bus Power System Using the Discrete Sliding Mode Control Technique. *Discrete Dyn. Nat. Soc.* **2018**, *2018*, 5758324. [CrossRef]
8. Muthana, T.A.; Mohamed, Z. Sliding Mode Control of Chaos in a Single Machine Connected to an Infinite Bus Power System. *Math. Probl. Eng.* **2018**, *2018*, 2703684. [CrossRef]
9. Njah, A.N. Tracking control and synchronization of the new hyperchaotic Liu system via backstepping techniques. *Nonlinear Dynam.* **2010**, *61*, 1–9. [CrossRef]
10. Yu, Y.; Zhang, S. Controlling uncertain Lu system using backstepping design. *Chaos Soltions Fractals.* **2003**, *15*, 897–902.
11. Mohammad, A.; Arash, K.; Behzad, G. Control of chaos in permanent magnet synchronous motor by using optimal Lyapunov exponents placement. *Phys. Lett. A* **2010**, *374*, 4226–4230.
12. Yassen, M.T. The optimal control of Chen chaotic dynamical system. *Appl. Math. Comput.* **2002**, *131*, 171–180. [CrossRef]
13. Zhang, F.; Chen, R.; Chen, X. Analysis of a Generalized Lorenz–Stenflo Equation. *Complexity* **2017**, *2017*, 7520590. [CrossRef]
14. Li, Y.; Zhao, Y.; Yao, Z. Chaotic Control and Generalized Synchronization for a Hyperchaotic Lorenz–Stenflo System. *Abstr. Appl. Anal.* **2013**, *2013*, 515106. [CrossRef]
15. Hsu, K.C. Variable Structure Control Design for Uncertain Dynamic Systems with Sector Nonlinearities. *Automatica* **1998**, *34*, 505–508. [CrossRef]
16. Yan, J.J. Sliding Mode Control Design for Uncertain Time-Delay Systems Subjected to a Class of Nonlinear Inputs. *Int. J. Robust Nonlin. Contr.* **2003**, *13*, 519–532. [CrossRef]
17. Li, H.; Liao, X.; Lei, X. Two fuzzy control schemes for Lorenz–Stenflo chaotic system. *J. Vib. Control.* **2012**, *18*, 1675–1682. [CrossRef]
18. Deeborah, H.H.; Andrew, M.G.; William, G.M. *Calculus Single and Multivariable 4th Edition with Study Guide*; John & Wiley and Son: Hoboken, NJ, USA, 2015.